JMEPEG (1992) 1:823-830

Stress-Corrosion Cracking of 15Cr-15Ni-2.2Mo Titanium-Modified Austenitic Stainless Steels

H. Shaikh, S. Venkadesan, C. Narayanan, H.S. Khatak, and J.B. Gnanamoorthy

The stress-corrosion cracking (SCC) behavior of two alloys of titanium-modified austenitic stainless steels with different Ti/C ratios in the 20% cold worked condition was studied in 45% boiling magnesium chloride (BP 427 K) using the constant-extension rate testing (CERT) technique. The SCC susceptibility of the two titanium-modified alloys was assessed using the ratios of the values of ultimate tensile strength (UTS) and percent elongation in magnesium chloride and liquid paraffin, the susceptibility index (I), crack propagation rates (CPR), and stress ratios at different values of plastic strains. The results obtained on these alloys were compared with AISI type 316 stainless steel. It was observed that the two titanium-modified austenitic stainless steels had better SCC resistance than type 316 stainless steel, mainly due to their higher nickel content and, to a lesser extent, to the presence of titanium. Increasing the value of the Ti/C ratio led to increased SCC resistance due to the availability of more free titanium in the solid solution. Fractography of the failed samples indicated failure by a combination of transgranular SCC and ductile fracture.

1. Introduction

THE success of a liquid metal fast breeder reactor as a commercially viable power-producing plant depends, to a great extent, on improving the fuel burn-up, which is limited by void swelling. Void swelling produces dimensional changes in the wrapper of the subassemblies and thus gives rise to difficulties in loading and unloading operations. Hence, the development of low-swelling materials for in-core applications gains paramount importance. Apart from void swelling resistance, materials for such applications should possess good elevated temperature mechanical properties, excellent corrosion resistance in liquid sodium, and adequate resistance to radiation damage. Therefore, austenitic stainless steels, such as type 316, are used as fuel cladding and wrapper materials. The performance of these materials is quite adequate considering that the fuel assemblies are subjected to an accumulated dose of approximately 65 displacements per atom (dpa).[1] However, for an economically viable commercial fast breeder reactor, materials with improved swelling resistance at damage levels greater than 100 dpa would be required. Control of chemical composition, cleanliness of the steel, and cold work could help in meeting the above requirement.[2,3]

In view of the above requirement, a titanium-modified 15Cr-15Ni-2.5Mo austenitic stainless steel, also called Alloy D-9, conforming to ASTM A 771 (UNS S38660) is considered as a candidate material for clad and wrapper tube applications.[1] Although the effectiveness of additions of titanium to improve the resistance to void swelling and irradiation creep is connected with the existing carbon content, the role of the Ti/C ratio is not yet clear.[4] Hence, work on low-swelling titanium-modified austenitic stainless steels with emphasis on the role of the Ti/C ratio was initiated. Microstructural and high-temperature mechanical properties of these stainless steels were reported previously.[5]

In stabilized stainless steels, such as AISI type 321 and 347, titanium or niobium is added to stabilize the stainless steel against $Cr_{23}C_6$ precipitation by promoting the precipitation of TiC or NbC. This thus leads to enhanced resistance to sensitization for the stabilized grades compared to the nonstabilized grades. Increasing the value of the Ti/C ratio leads to increasing sensitization resistance. The effect of titanium and consequently the Ti/C ratio on the stress-corrosion cracking (SCC) resistance of these stabilized steels is not well understood.

Available literature suggests that SCC resistance varies with the environment. Latanision *et al.*[6] reported a decrease in the stress-corrosion cracking resistance in hot concentrated chloride solution with increasing addition of titanium to the stainless steel. Also, increasing the carbon content of the steel increased the stress-corrosion cracking resistance in this environment.[7] On the contrary, in high-temperature high-purity water, an increase in carbon was found to decrease stress-corrosion cracking resistance. In high-temperature high-purity water, titanium additions were reported to increase the stress-corrosion cracking resistance of the stainless steel by decreasing the carbon content of the austenitic matrix.[7]

In the present investigation, the stress-corrosion cracking susceptibility of cold worked D-9 alloy was evaluated. A comparison was made with the SCC resistance of cold worked AISI type 316 stainless steels.[8] An attempt is made to evaluate the role of titanium and the Ti/C ratio on the SCC resistance of the D-9 alloy by studying alloys with two different Ti/C ratios.

2. Experimental

Rod made of two D-9 alloys (see Table 1 for compositions) was solution annealed at 1123 K for 25 min, followed immediately by heating at 1143 K for 5 min. These rods were then cold

H. Shaikh, S. Venkadesan, C. Narayanan, H.S. Khatak, and **J.B. Gnanamoorthy,** Metallurgy and Materials Programme, Indira Gandhi Centre for Atomic Research, Kalpakkam, India.

Table 1 Chemical Compositions of Two Commercial Scale Heats of Alloy D-9 and AISI Type 316 Stainless Steel

Element	Composition, wt% Heat 1	Heat 2	Type 316[8]
C	0.0523	0.0522	0.05
Mn	1.507	1.509	1.2
Si	0.495	0.505	0.38
S	0.0033	0.0025	0.011
P	0.011	0.011	0.026
Cr	15.095	15.068	15.56
Ni	15.037	15.068	12.59
Mo	2.261	2.248	2.27
Ti	0.211	0.315	...
B	0.001	0.001	...
Co	0.015	0.015	...
Ta + Nb	0.02	0.02	...
N	0.006	0.0066	0.043
Fe	bal	bal	bal
Ti/C ratio	4	6	...

Table 2 Tensile Properties of Two D-9 Alloys in Liquid Paraffin at 427 K

Ti/C ratio	Yield strength, MPa	Ultimate tensile strength, MPa	Fracture stress, MPa	Elongation, %
4	658	680	438	21
6	676	712	451	17

swaged by 20%. Round tensile specimens with a gage diameter of 2.5 mm, as shown in Fig. 1, were machined from these rods. These samples were pulled in tension at a constant extension rate of 0.05 mm/min (initial strain rate = 8.3×10^{-5}/s) in an Instron model 1122 machine in an inert medium of liquid paraffin at 427 K and a corrosive environment of boiling 45% $MgCl_2$ solution (BP 427 K). Optical microscopy of the samples before and then after testing by SCC was then carried out to study the microstructure and the stress-corrosion cracking failure mode of these samples. Fractographic features were studied in greater detail in a scanning electron microscope (SEM).

3. Results and Discussion

The load-elongation curves obtained in liquid paraffin and in magnesium chloride were evaluated to determine the yield stress (YS), ultimate tensile stress (UTS), fracture stress (FS), and ductility. The results of the mechanical-property evaluation are given in Table 2. The D-9 alloy with the Ti/C ratio of 6 had higher yield strength, ultimate tensile strength, fracture stress, and lower ductility than the steel with a Ti/C ratio of 4.

The stress corrosion susceptibility of the two austenitic alloys was evaluated, and the results were compared with those of type 316 stainless steel with a maximum cold work of 15%. Cold work[8] is reported to decrease the SCC resistance of austenitic stainless steel, because it increases the defect density and thus decreases the time to crack initiation.[7] Because type 316 stainless steel is of the stable variety, no strain-induced martensite is expected to form on cold working at room temperature. Thus, the reported beneficial effect of deformation-induced martensite on SCC[7] is not expected on further cold

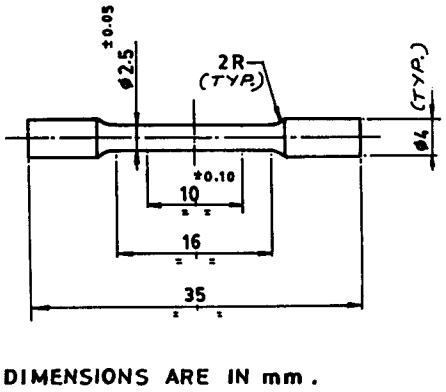

Fig. 1 Schematic of tensile samples.

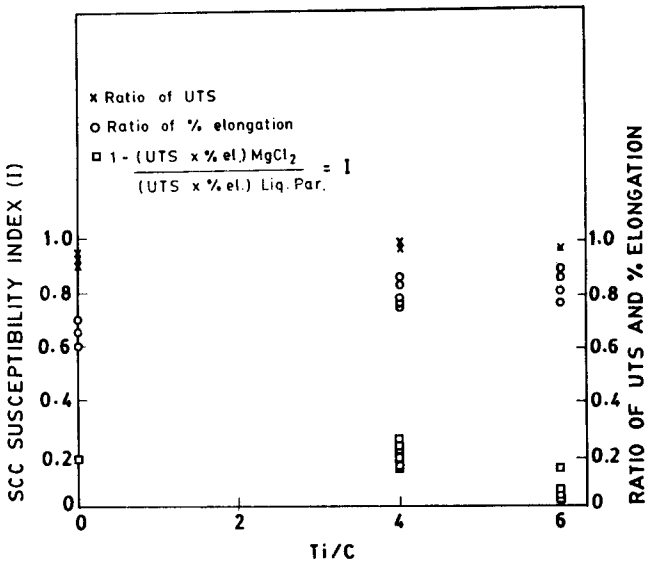

Fig. 2 Dependence of various SCC susceptibility parameters on Ti/C ratio. The SCC results of 15% cold worked type 316 stainless steel are indicated at Ti/C = 0.

working of type 316 stainless steels, and hence, its SCC properties could be expected to only further degrade with cold work in excess of 15%.

Figure 2 illustrates the values of SCC susceptibility evaluated by comparing the values of ultimate tensile strength and percentage elongation in magnesium chloride and in liquid paraffin and by using the susceptibility index (I), proposed by Hishida *et al.*,[9] which is given by the equation:

$$I = 1 - \frac{(\text{UTS} \times \%\text{elongation})_{MgCl_2}}{(\text{UTS} \times \%\text{elongation})_{\text{liquid paraffin}}}$$

The evaluation based on the ratio of the values of ultimate tensile strength in magnesium chloride and in liquid paraffin indicated that there was no significant variation in SCC susceptibility with increasing Ti/C ratio, whereas the ratio of percentage elongation suggested only a slight improvement in

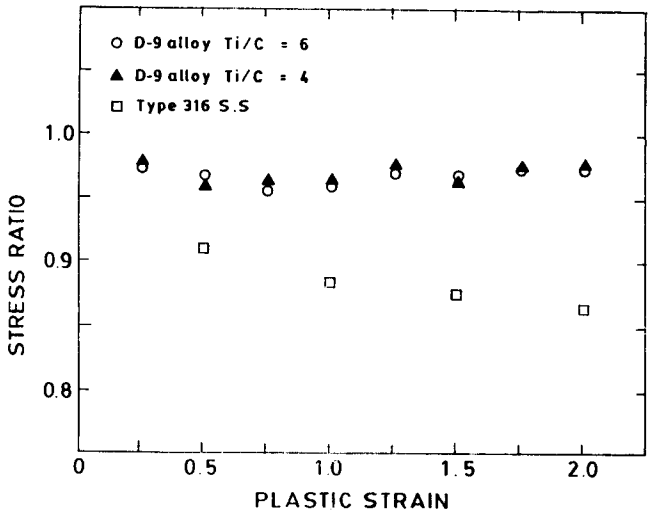

Fig. 3 SCC susceptibility of two D-9 alloys and type 316 stainless steel, as indicated by variation in the stress ratio with plastic strain.

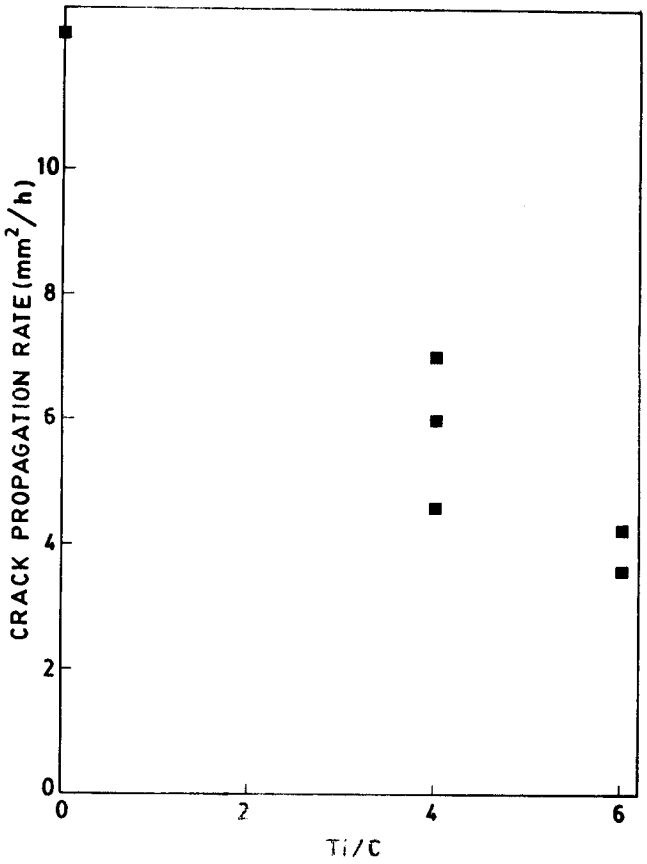

Fig. 4 Variation of the crack propagation rate with Ti/C ratio. Crack propagation rate of type 316 stainless steel is included at Ti/C = 0.

SCC resistance with increasing Ti/C ratio. The use of the cracking index as an assessment criteria indicated an improvement in the SCC resistance only when the Ti/C ratio increased from 4 to 6. The use of the above assessment parameters suggested that neither Ti nor Ti/C ratio had any significant effect on the SCC resistance of D-9 alloys and that there was not much to choose between type 316 stainless steel and the D-9 alloy from the SCC standpoint. Khatak *et al.*[8] and Kim *et al.*[10] expressed scepticism on the use of the constant-extension rate testing (CERT) technique for assessing the SCC susceptibility of materials with widely differing mechanical properties and microstructures. They stated that selection of the proper assessment parameters was important in the precise prediction of SCC behavior. Khatak *et al.*[8] argued that SCC damage, calculated in terms of the ratios of the values of ultimate tensile strength, percent elongation (in $MgCl_2$ and in liquid paraffin), and the cracking index, will depend on the time the specimen spent in the corrosive environment before fracture. In the case of less ductile materials, the time-to-failure and hence the time for crack growth by SCC decreases correspondingly.

The scepticism expressed in the use of the CERT technique could be overcome by assessing the damage with parameters that could account for the time the material spent in the corrosive environment. Maiya *et al.*[11] suggested the use of the stress ratio at various plastic strain values as an appropriate indicator of the SCC susceptibility of materials with varying microstructural and tensile properties. Figure 3 is a plot of the ratio of stress, in magnesium chloride and in liquid paraffin, at various plastic strain values. The data suggest a much higher susceptibility (compared to the assessment parameters in Fig. 2) for type 316 stainless steel with respect to the two D-9 alloys. Figure 3 also reveals very little difference in SCC resistance between the two D-9 alloys with varying Ti/C ratio.

The observed trend in SCC susceptibility, based on the use of the stress ratio, was further verified by calculating the crack propagation rate (CPR) for the three alloys by using the equation proposed by Desestret and Oltra.[12] According to their equation, CPR = S_c/t_f mm²/s, where S_c is the SCC area, and t_f is the time-to-failure. The time-to-failure was considered the time spent by the material between the yield strength and the maximum load in $MgCl_2$ solution. The lower limit used to calculate the time-to-failure was fixed as yield strength, as little difference was observed among its values in the tests carried out in liquid paraffin and in boiling $MgCl_2$. Because the material undergoes only pure ductile failure beyond maximum load in $MgCl_2$, the maximum load was considered the upper limit used to calculate the time-to-failure. The SCC area of the cross section was calculated based on the engineering stress at fracture, using the equation:

$$S_c = S_o \times (1 - R_c/R)$$

where S_c is the stress corrosion area, S_o is the original area of cross section, R_c is the fracture stress in $MgCl_2$, and R is the fracture stress in liquid paraffin. Thus, the final form of the

equation suggested that the ratio of the fracture stress was indicative of the total percentage of the ductile area present on the fracture surface. Figure 4, which shows the variation in the crack propagation rate with Ti/C ratio, indicates a significant drop in the crack propagation rate of the two 20% cold worked D-9 alloys compared to that of 15% cold worked type 316 stainless steel. The difference observed in the SCC resistance of the two D-9 alloys based on crack propagation rate was much larger than that observed while using the other assessment parameters in Fig. 2 and 3. The studies of Khatak *et al.*[13] and Shaikh *et al.*[14] have shown that the trends obtained by the calculation of the crack propagation rate using the results of the CERT technique are more reliable than the assessment parameters used in Fig. 2, and are even more so when material with varying strength levels, ductilities, and microstructures were involved. In fact, their crack propagation rate results showed trends that matched the constant-load results performed at a certain fraction of the yield strength.

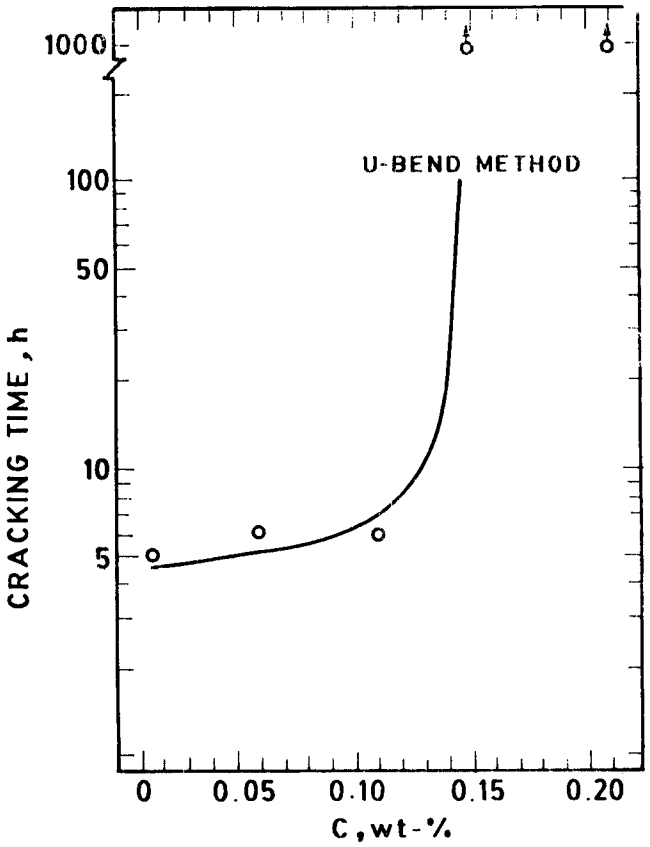

Fig. 5 Effect of carbon on the SCC susceptibility of 18-10 stainless steel in boiling 45% magnesium chloride.[7]

Hanninen[7] reported that the SCC resistance of stainless steels with carbon contents greater than 0.1% was high in hot chloride solution (Fig. 5), whereas below that value the carbon content had very little effect. In the present study, the carbon content of the two D-9 alloys and type 316 stainless steel was about 0.05%. Hence, carbon was expected to play a minimal role. The crack propagation rate of the two D-9 alloys was found to be two to three times lower than that of type 316 stainless steel. This improvement in SCC resistance of the D-9 alloys could have been due to two factors—higher nickel content and the presence of titanium in the D-9 alloys.

The effect of nickel in improving the SCC resistance of austenitic alloys is well documented by the well-known Copson's curve.[7] The effect of nickel in improving the SCC resistance of an austenitic alloy has been attributed to its effect on increasing the stacking fault energy (SFE). Alloy D-9 is reported to behave as a high stacking fault energy material, based on tensile and microstructural examinations.[5]

Latanision *et al.*[6] reported a deterioration in SCC resistance in hot chloride solution, on addition of titanium to the stainless steel. Hanninen[7] stated that this drop in SCC properties on addition of titanium could be due to lowering of the free carbon content of the steel to a more susceptible range by the formation of TiC. This suggested that increasing the Ti/C ratio was detrimental to SCC resistance. On the contrary, the present results (Fig. 2, 3, and 4) suggested that increasing the Ti/C ratio did not appear harmful, and instead, a slight improvement in the resistance of the D-9 alloys with increasing Ti/C ratio was observed. This could probably have been due to the lower carb-

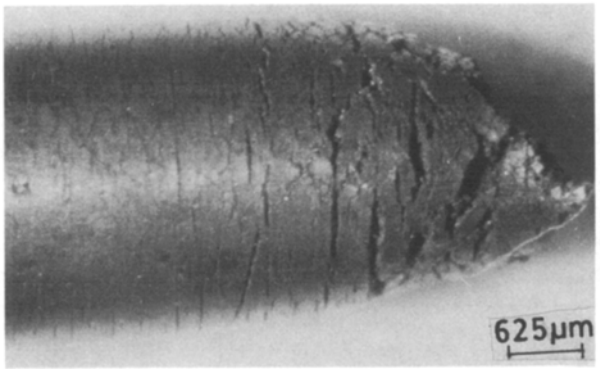

(a)

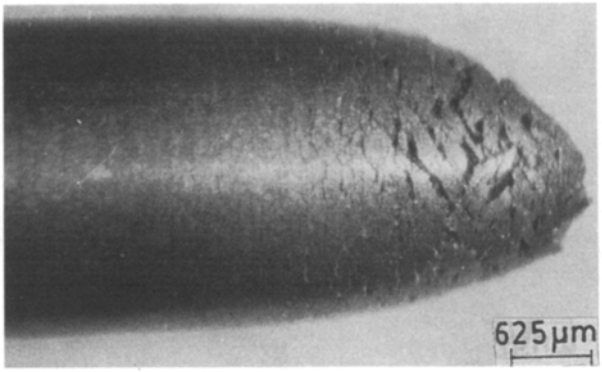

(b)

Fig. 6 Stereomicrographs of the cross section perpendicular to the fracture surface. **(a)** Ti/C = 4. **(b)** Ti/C = 6.

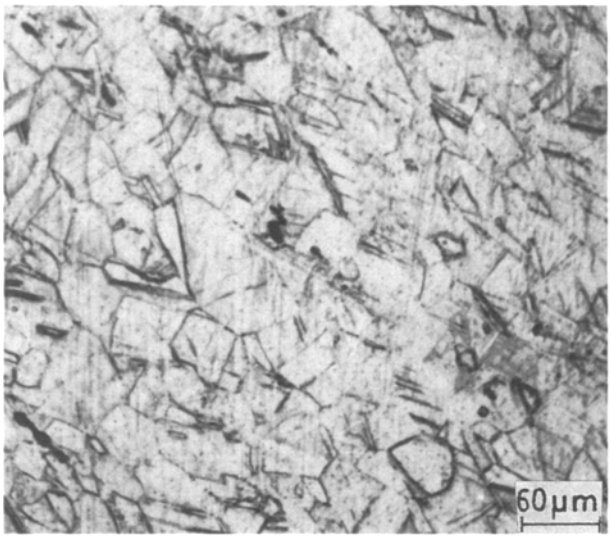

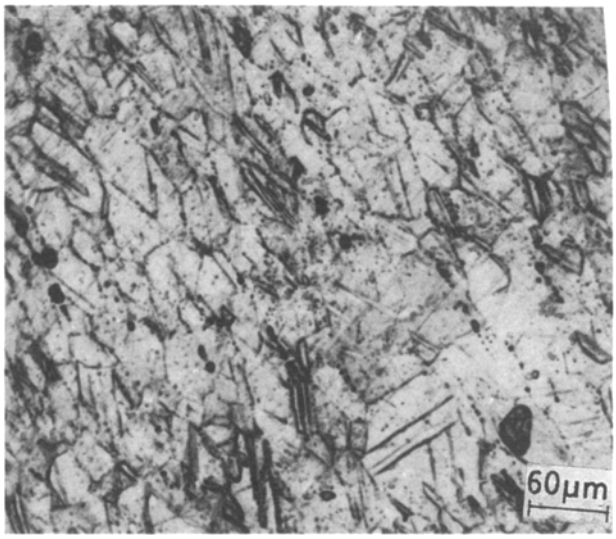

Fig. 7 Microstructures of the D-9 alloys. **(a)** Ti/C = 4. **(b)** Ti/C = 6.

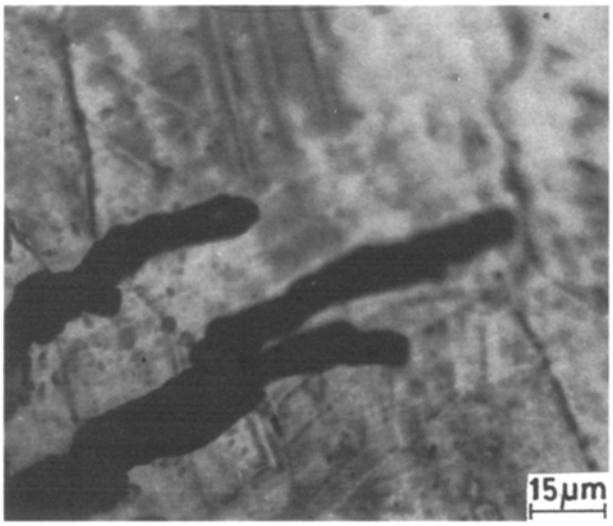

Fig. 8 Typical micrograph showing TGSCC in the austenite matrix of the D-9 alloys.

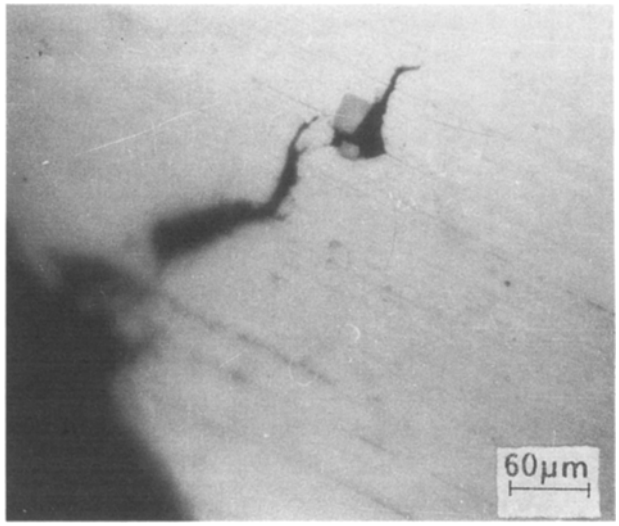

Fig. 9 Typical micrograph of an as-polished specimen showing a crack propagating around a TiCN particle in the D-9 alloy.

on content of the alloys used in the present study. The carbon content was already in the most susceptible range of SCC,[7] and further lowering of the carbon content as a result of TiC formation would not have contributed significantly to SCC resistance. Thus, improvement in SCC properties with increasing Ti/C ratio could be related only to the increased amount of free titanium available in the matrix.

From the above arguments, it could be inferred that the higher SCC resistance of the 20% cold worked D-9 alloy compared to the 15% cold worked type 316 stainless steel is a consequence of the increased nickel content and titanium addition. The dramatic improvement in the SCC resistance of the D-9 alloy over type 316 stainless steel and the marginally higher SCC resistance of the alloy with the higher Ti/C ratio suggested that the effect of the high nickel content was more pronounced than the presence of titanium.

Figures 6(a) and (b) are stereomicrographs of the cross section perpendicular to the fracture surface. The D-9 alloy with the lower Ti/C ratio had more numerous and deeper secondary cracks, consistent with the higher susceptibility of this alloy to SCC.

Figures 7(a) and (b) show the microstructures of the two D-9 steels. A substantial number of mechanical twins caused by cold working are visible. Note also that the steel with the Ti/C ratio of 4 has a slightly larger grain size than the steel with the Ti/C ratio of 6. This difference in grain size could also have

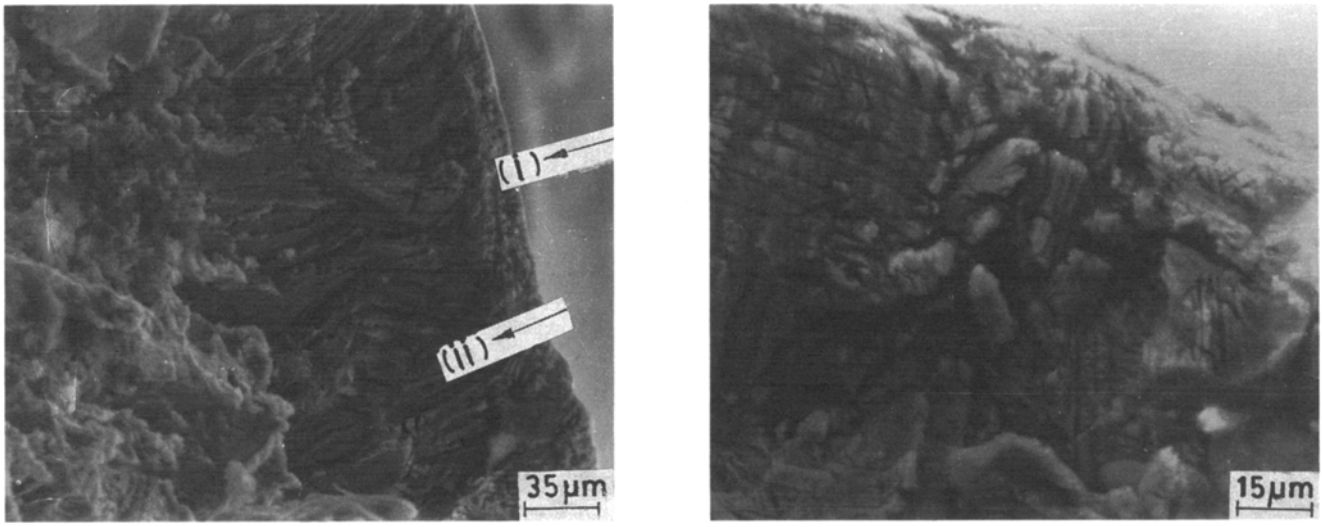

Fig. 10 Fractographs showing **(a)** TGSCC + ductile failure and **(b)** region I in Fig. 10(a).

contributed to the increase in SCC resistance of alloy with the higher Ti/C ratio.

The crack morphology in both the steels was of the transgranular type. A typical example is shown in Fig. 8, and Fig. 9 is a typical micrograph showing a propagating crack in an as-polished specimen. Note that wherever the crack encounters cuboidal second-phase particles, it runs along the precipitate boundary rather than crack through it. In an earlier investigation[15] on the two D-9 alloys, the cuboidal particles were identified as TiCN. The cuboidal TiCN phases formed during solidification of the steel. These phases appear as large cuboids and thus cannot be refined during annealing, because they have a higher melting point than the matrix alloy. Because these particles are nondeformable, their sizes depend essentially on the cooling rate during solidification. The nondeformability of these particles causes the arrest of the crack wherever it encounters these particles. Further application of load causes increasing dislocation pile-up at the crack tip, leading to a stress concentration and resultant interfacial dissolution.

Figure 10 shows the typical morphologies observed in the SCC region of the fracture surface of both the D-9 alloys. These SEM fractographs clearly indicate that failure occurred by a combination of transgranular stress-corrosion cracking (TGSCC) (regions I and II) and ductile failure, as shown in Fig. 10(a). Region I, which is the area around the initiation point shown in Fig. 10(a), is magnified in Fig. 10(b). The fractographic features at the initiation point are not typical of TGSCC and as well defined as those in the regions of propagation (region II in Fig. 10a).

4. Conclusions

The stress-corrosion cracking resistance of the two 20% cold worked D-9 alloys was found to be better than that of 15% cold rolled type 316 stainless steel. This improvement in SCC resistance was attributed mainly to the higher nickel content in the D-9 alloys, although titanium content and the Ti/C ratio also played a role. The D-9 alloy with the higher Ti/C ratio was found to be more resistant than the alloy with the lower Ti/C ratio. The stress-corrosion cracking mode was found to be transgranular.

Acknowledgments

The authors wish to acknowledge the support received from their colleagues K. Shanmugam, S. Venugopal, Jr., and C. Radhika for their valuable help during the course of the work.

References

1. P. Rodriguez and S.L. Mannan, *Ind. J. Technol.*, Vol 28, 1990, p 281.
2. W.G. Jhonstone, T. Lauritzer, J.H. Rosolowski, and A.M. Turkalo, *Proc. Sem. Radiation Damage in Metals*, American Society for Metals, 1973, p 227.
3. J.O. Steigler and E.E. Bloon, *J. Nucl. Mater.*, Vol 41, 1971, p 341-344.
4. C.V. Sundaram, P. Rodgriguez, and S.L. Mannan, *J. Inst. Eng. (Ind.)*, Vol 67, 1986, p 1-11.
5. S. Venkadesan, P.V. Sivaprasad, M. Vasudevan, S. Venugopal, and P. Rodriguez, *Trans. Ind. Inst. Met.*, Vol 45, 1992, p 57-68.
6. R.M. Latanision and R.W. Staehle, *Proc. Conf. Fundamental Aspects of Stress Corrosion Cracking*, NACE, 1969, p 214-307.
7. H.E. Hanninen, *Int. Met. Rev.*, Vol 24, 1979, p 85-135.
8. H.S. Khatak, P. Muraleedharan, J.B. Gnanamoorthy, and P. Rodriguez, *J. Nucl. Mater.*, Vol 168, 1989, p 157-161.
9. M. Hishida and H. Nakada, *Corrosion*, Vol 33, 1977, p 332-338.
10. C.D. Kim and B.E. Wilde, *Stress Corrosion Cracking—The Slow Strain Rate Technique*, ASTM STP 665, 1979, p 97-112.

11. P.S. Maiya, W.J. Shack, and T.F. Kassner, *Corrosion*, Vol 46, 1990, p 954-963.
12. A. Desestret and R. Oltra, *Corr. Sci.*, Vol 20, 1980, p 799-820.
13. H.S. Khatak, P. Muraleedharan, J.B. Gnanamoorthy, P. Rodriguez, and K.A. Padmanabhan, Poster Session Papers, *6th Int. Conf. Fracture* (New Delhi), 1984, p 153-157.
14. H. Shaikh, H.S. Khatak, S.K. Seshadri, J.B. Gnanamoorthy, and P. Rodriguez, *Metall. Trans. A*, in press.
15. S. Venkadesan, A.K. Bhaduri, P. Rodriguez, and K.A. Padmanabhan, *J. Nucl. Mater.*, Vol 186, 1992, p 177-184.